Article:
Real, DA, Hoffmann, S, Leonardi, D et al. (2 more authors) (2021) A quality by design approach for optimization of Lecithin/Span® 80 based nanoemulsions loaded with hydrophobic drugs. Journal of Molecular Liquids, 321. 114743. ISSN 0167-7322

https://doi.org/10.1016/j.molliq.2020.114743

A quality by design approach for optimization of Lecithin/Span® 80 based nanoemulsions loaded with hydrophobic drugs.

Daniel A. Real,[a,b&] Stefan Hoffmann Stefan,[c&] Darío Leonardi,[a,b] Francisco M. Gooycolea,[c,d*] Claudio J. Salomon[a,b*]

[1]Instituto de Química de Rosario, Consejo Nacional de Investigaciones Científicas y Tecnológicas, Suipacha 531, 2000, Rosario, Argentina.

[2]Departamento Farmacia, Facultad de Cs. Bioquímicas y Farmacéuticas, Universidad Nacional de Rosario, Suipacha 531, 2000, Rosario, Argentina.

[3]Institute of Plant Biology and Biotechnology (IBBP), Westfälische Wilhelms-Universität Münster, Schloßplatz 8, 48143 Münster, Germany

[4]School of Food Science and Nutrition. University of Leeds. Woodhouse Ln. Leeds, LS2 9JT, United Kingdom

[&]*Authors contributed equally to this work.*

*Corresponding author:

Claudio J. Salomon. Pharmacy Department, Faculty of Pharmaceutical and Biochemical Sciences, National University of Rosario, Suipacha 531, 2000, Rosario, Argentina; email address: csalomon@fbioyf.unr.edu.ar

Date of acceptance: 17 November 2020

Journal of Molecular Liquids 321 (2021) 114743

https://doi.org/10.1016/j.molliq.2020.114743

GRAPHICAL ABSTRACT

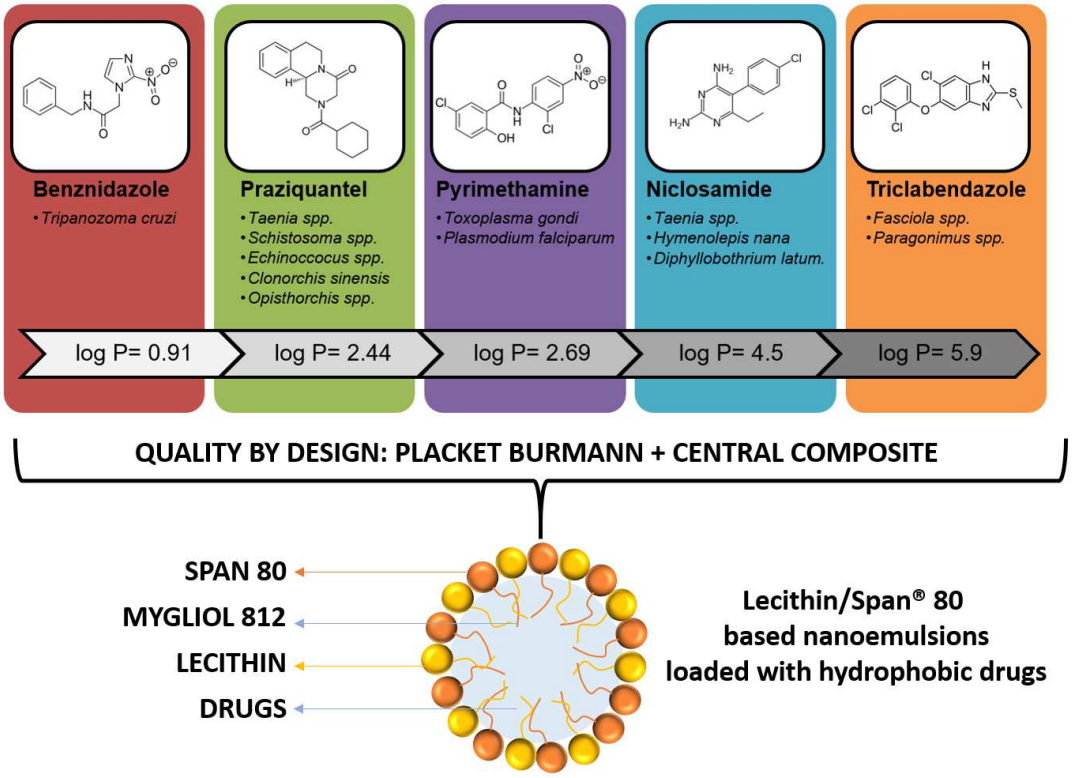

ABSTRACT

Lately, nanoemulsions loaded with hydrophobic drugs have been successfully developed to improve the treatment of several global diseases. On this subject, a detailed study of the crucial role of the excipients and the experimental conditions used for these nanosystems is still required. Thus, the aim of this work was the development of nanoemulsions of Benzidazole (Class I, log P=0.91), Praziquantel (Class II, log P=2.44), Pyrimethamine (Class II/IV, log P=2.69), Niclosamide (Class II/IV, log P=4.5), and Triclabendazole (Class II/IV, log P=5.9) using Span® 80, soybean lecithin and Miglyol® 812 as excipients. A Placket-Burman design was selected to identify the main parameters that influence in the desirable characteristics of such formulations. Then, a full factorial design was built to analyze the effect of the factors identified in the screening phase. Plackett-Burman design indicated that Miglyol® 812 and lecithin were the two most influencing factors on the hydrodynamic diameter of the systems. In addition, the association efficiency was influenced by the log P of each drug while the response stability in PBS was modified by Span® 80 and log P. The results of the full factorial design revealed that concentration of Miglyol® 812 and log P values of each drug have a remarkable impact on the stability of the nanosystems. The optimal conditions for the preparation of nanoemulsions were verified by other independent experiment and the results were in agreement with the predicted optimum values. Thus, this methodology could serve as an attracttive platform to deliver other hydrophobics compounds in stable nanoemulsions.

KEYWORDS: Nanoemulsions, Quality by Design, Placket Burmann, Central Composite, Lecithin, Span 80.

1. Introduction

One of the major challenges in the pharmaceutical industry is the design of novel drug delivery systems with improved biopharmaceutical properties[1]. However, the poor aqueous solubility of drugs may leads to a low/erratic bioavailability, affecting the *in-vivo* performance of such systems[2]. In this regard, several strategies have been explored to overcome such drawback including the supercritical antisolvent technique[3-5], amorphous and crystalline solid dispersions [6-8], cyclodextrin complexes[9-11], cosolvency[12-14] and microencapsulation[15-17]. Particularly, the reduction of the particle size from micro- to nanometer scale is as a valuable and widely applied approach to improve the apparent saturation solubility, dissolution rate and bioavailability of hydrophobic molecules[18]. Thus, nanoemulsions (NEs), which exhibit mean droplet diameters ranging from ~10 to ~1000 nm, are one of the most promising pharmaceutical platforms to deliver chemotherapeutic agents for the potential treatment of cancer[19]; neurodegenerative pathologies[20-22] and type II diabetes[23]. It is worth mentioning that NEs are conventionally prepared using high energy emulsification techniques (high-pressure homogenization or ultrasound methods) as well as low-energy emulsification methods (solvent displacement technique). In the case of the solvent displacement process, the immediate diffusion of the organic used solvent (acetone, ethanol, methanol, etc) into the external aqueous phase leads to the spontaneous formation of oil nanodroplets, stabilized by surface-active agents. In this regard, different surfactant agents including poloxamers, sodium lauryl sulphate, polysorbates, soybean lecithin[24-27] and the selected experimental conditions play a fundamental role toward the formulation of stable NEs with desire physicochemical properties[28-32]. Even though these systems have often improved the physicochemical properties of the loaded drugs,

it is necessary to increase the number of systematic evaluations related with the methodology to obtain a maximum association efficiency, stability and a minimum polydispersion index. Thus, many statistical experimental designs are useful techniques to collect a high number of data with fewer runs, which may allow a better control during the complex methodologies[31-34]. Following these "Quality by Design criteria", the aim of this work was the development of NEs loaded with Benznidazole, Praziquantel, Pyrimethamine, Niclosamide, and Triclabendazole. These widely prescribed drugs belong to Class II/IV into the Biopharmaceutical Classification System (BCS)[1]. Herein, for the first time, these NEs were prepared and optimized using an experimental design approach with Miglyol® 812 as oil phase and soybean lecithin and Span® 80 as co-surfactants. The nanoformulations were characterized in terms of particle size, zeta potential, association and loading efficiency, stability in biological media and storage stability. It is worth noting that these model drugs, used for the treatment of parasitic neglected tropical diseases, are included in the World Health Organization Model List of Essential Drugs[35].

2. Experimental

2.1 Materials

Benznidazole (BZN) (lot 260835, 99.45% purity) was a gift from Produtos Roche Químicos e Farmacéuticos S.A. (Sao Paulo, Brazil), Pyrimethamine (PYR), Niclosamide (NICLO) and Triclabendazole (TCBZ) were provided by Chemo (Buenos Aires, Argentina). Racemic Praziquantel (PZQ) (lot C19H24N2O2, purity > 99.4%) was purchased from Romikin (Buenos Aires, Argentina) Miglyol® 812 was kindly provided by Peter Cremer

Oleo (USA). The surfactant lecithin (Epikuron® 145v, a phosphatidylcholine enriched fraction of soybean lecithin) was kindly donated by Cargill (Spain). Span® 80 (lot B20Y9) was purchased from Saporiti (Buenos Aires, Argentina). All water used in the study was ultrapure MilliQ water with a resistivity of 18.2 MΩ at 25 °C and passed through a filter with a pore size of 0.22 μm. All other reagents used were of analytical grade if not specified otherwise.

2.2 Nanoemulsion formulation

The general procedure to prepare the NEs was based on a previous described protocol23,30. The amounts of the excipients and the experimental factors varied as indicated by the experimental designs. Briefly, an organic phase was formed by dissolving drugs, lecithin (Epikuron 145v, 0 – 120 mg) and Span 80 (0 – 2 % v/v) in an aliquot (0,5 – 3 mL) of the solvent (ethanol or acetone), followed by the addition of Mygliol 812 (0 – 350 μL) and adding solvent up to 10 mL. This 10 mL volume of organic phase were immediately mixed (0 - 500 rpm) with water following the order indicated by the design (O-W, W-O). NEs were formed spontaneously due to the organic solvents diffusion. Finally, after an indicated time (1 – 30 min) the solvent and part of the water were evaporated at 40˚C under vacuum on a R-210 Rotavapor (Büchi Labortechnik GmbH, Essen, Germany) to reach the final evaporation volume (7-10 mL).

2.3 Quality By Design experiments

For the screening phase, a Placket-Burman design (12 runs, 0 center points), was selected to identify the effect of 10 factors over 6 responses that influence the desirable characteristics of Lecithin/Span NEs[34]. The studied parameters were excipient

concentrations (Miglyol® 812; lecithin; Span 80), solvent (Ethanol and Acetone), stirring rate (0 – 500 rpm), mixing order (O-W, W-O), time before evaporation (1 – 30 min), aqueous volume (10 – 20 mL) and final evaporation volume (7 – 10 mL). The different responses analyzed were drug association efficiency, particle size (Z-average hydrodynamic diameter), PDI, derived count rate, particle size stability over time (30 days) and stability in PBS. TCBZ (log P = 5.9) and BZN (log P = 0.91) were used as model drugs in this phase. The detailed experimental design was shown in Table 1.

To further refines the analysis of the influence of the main parameters identified in the screening phase, a Central Composite design (4 factors, 6 responses) was implemented. This factorial design consisted of 30 experiments, which included combinations of the selected factors in the following ranges: Miglyol® 812, 0-350 µL, lecithin 0-120 mg, Span® 80 1-3% v/v and log P values 1.6-5.9. Taking into account the results of the screening phase several factors were fixed. Thus, time before evaporation were set to 1 min, aqueous phase volume and final evaporation volume was set to 20 mL and 10 mL respectively. Mixing order was set O-W and the stirring was set to 0 rpm. The detailed experimental design was shown in Table 3.

2.4 Physicochemical characterization

The nanosystems were characterized regarding their size (Z-average hydrodynamic diameter), polydispersity (PDI), derived count rate (DCR) and zeta-potential (ZP). The particle size distribution and polydispersion index were determined by dynamic light scattering with non-invasive back scattering (DLS-NIBS) with a measurement angle of 173°. The autocorrelation functions were fitted with the default Non-Negative Least

Squares (NNLS) fit to calculate the intensity size distribution plots and evaluate the Z-average hydrodynamic diameter. The zeta-potential was measured by mixed laser Doppler velocimetry and phase analysis light scattering (M3-PALS). A Malvern Zetasizer NanoZS (Malvern Instruments, Malvern, UK) fitted with a red laser (λ=632.8 nm) was used for both determinations. Samples were diluted 1:100 and, then, the measurements were carried out in triplicate. The Zeta Sizer Software (v 7.12) was used to acquire and evaluate the size and zeta potential data.

2.5 Association and loading efficiency

The nanoformulations were separated from the insoluble solids in suspension by ultracentrifugation (Mikro 220 R, Hettich GmbH & Co. KG, Tuttlingen, Germany) at 25,000 x g for 10 minutes at 15 °C. The nanoformulations formed a creamy layer on top of the aqueous phase, while the suspended crystals precipitated forming a pellet at the bottom of the vial. The amount of drug in the nanoformulations was determined by HPLC using an UV detector against a standard curves produced with drugs stock solution. The association efficiency was calculated as the difference between the total amount of drug incorporated in the NEs and the amount present in the filtrate and the pellet (Equation 1):

$$Association\ efficiency\ (\%) = \frac{Mass\ drug_{associated}}{Mass\ drug_{theoretical}} * 100 \quad (1)$$

High Performance Liquid Chromatography with Ultraviolet/Light Detection (HPLC/UV-VIS) Analysis

The quantification of the drugs was performed using high performance liquid chromatography (HPLC). The analysis were performed with a Jasco HPLC system (JASCO

Labor-und Datentechnik GmbH; Gross-Umstadt; Germany) consisting of a 3-line degasser (DG-2080-53), a ternary gradient unit (LG-2080-02S), a semi-micro HPLC pump (PU-2085Plus), an autosampler (X-LC™ 3159AS), an intelligent column thermostat (CO-2060Plus) equipped with a C18 reversed-phase column 150 mm × 2.1 mm with a particle size of 2.6 µm. A fixed flow rate of 0.2 mL/min at T = 40 °C was used and 5-µL of sample were injected within a total run time of 10 min. The concentrations of the model drugs were detected using a UV/VIS detector (X-L™ 3075UV). All experiments were performed in triplicate.

2.6 Size stability in biological media

The stability of NEs during incubation in phosphate buffered saline (PBS, pH 7.4, at 37 °C) was studied based on the ratio between the particle size at 0 and 24 h (Equation 2):

$$PBS_{stability} = \frac{Size_{24h}}{Size_{0h}} \qquad (2)$$

2.7 Size stability over time

The systems were storage for 30 days at 25 °C and the storage stability (ST30) of NEs was evaluated in terms of the particle size at 0 and 30 days of storage (Equation 3):

$$ST_{30} = \frac{Size_{30d}}{Size_{0d}} \qquad (3)$$

2.8 Software

The software applied to the experimental design and ANOVA test was Design Expert version 7.0.3 (Stat-Ease Inc., Minneapolis, MN, USA).

3. Results and discussion

3.1 Screening phase

A Placket-Burman design was selected to screen and identify the main parameters that influence the desirable characteristics of the formulations[34]. The different responses analyzed were drug association efficiency, particle size (Z-average hydrodynamic diameter), PDI, derived count rate, particle size stability over time (30 days) and stability in PBS (Table 1). TCBZ (log P = 5.9) and BZN (log P = 0.91) were used as model drugs in this phase.

Insert Table 1

The results of the screening analysis are shown in Table 2. Of note, Miglyol® 812 and lecithin were the more influencing factors for the particle size, while Miglyol® 812, solvent, Span® 80, time before evaporation and mixing order were the factors influencing the PDI. Miglyol® 812, solvent and mixing order also modified DCR, whereas the log P of the drugs influenced the association efficiency. It is also important to note that Span® 80 and log P influenced the response stability in PBS, while both aqueous volume and final evaporation volume modified the stability over time. Finally, the stirring rate did not reach statistically significant effect over the studied responses.

Insert Table 2

Regarding the influence of the solvents in the organic phase, acetone increased the PDI when compared to ethanol (Fig. 1 A and 1B). It is in agreement with the Marangoni effect, which describes certain perturbation at the droplet interface occurring in the

emulsification step, probably due to a transfer of ethanol across the unequilibrated solvent/water interface. Herein, the surface activity of ethanol, as a consequence of its molecular interactions with organic solvents and water (dipole–dipole forces and hydrogen bonds, respectively), is higher than the surface activity of acetone leading, as a consequence, to a smaller PDI. This finding is in agreement with the literature. As reported, the concentration of ethanol, as cosolvent, played a fundamental role to control the PDI during the preparation of nanospheres through the emulsification–diffusion process[36]. Moreover, the mixing order influenced PDI and DCR while lowest PDI and highest DCR were obtained when mixing order was O-W (Fig. 1C and 1D). This fact could be due to the diffusion rate of the solvent. In case of O-W the diffusion rate is faster, reducing the PDI[37].

Insert Figure 1

As seen in Fig. 1E, the size stability in PBS was improved by increasing the amount of Span® 80 added to the NEs. It could be due to a decrease of the droplet coalescence rate by altering the optimum curvature of the surfactant layer (altering the interfacial tension). It is in accordance with the work of Rao and McClements[38], who described the formulation of stable NEs by using ionic and non-ionic surfactant agents. As shown in Fig. 1F and 1G, Miglyol® 812 content modified PDI and increased size, therefore, the optimization of this factor was carried out. Lecithin concentration did not modify, in a significant manner, the PDI but mainly affected the droplet size (Fig. 1H).

3.2 Full factorial design

To further refines the analysis of the influence of the main parameters identified in the screening phase, a full factorial design was implemented[39]. The model drugs selected for this analysis present a wide range of log P values, which are adequate for our purposes. The previously identified factors Miglyol® 812, lecithin, and Span® 80 were also analyzed (Table 3).

Insert Table 3.

The procedure was carried out using response surface methods (RSM) in order to estimate the values of the most important factors. It could lead to the best compromise between maximum association efficiency and DCR; in addition to a minimum PDI, size and zeta-potential, which appeared mostly influenced by the studied factors in the screening phase. The factorial design consisted of 30 experiments, which included combinations of the selected factors in the following ranges: Miglyol® 812, 0-350 µL, lecithin 0-120 mg, Span® 80 1-3% v/v and log P values 1.6-5.9 (Table 2). Taking into account the results of the screening phase (see above) several factors were fixed. Thus, time before evaporation were set to 1 min, because using this value the PDI was minimized (Figure 2A). Aqueous phase volume and final evaporation volume was set to 20 mL and 10 mL respectively, to increase the stability over storage (Figure 2B and 2C). Mixing order was set O-W, due to this methodology produced the smallest PDI and the

highest DCR (Figure 1C and 1D), and the stirring was set to 0 rpm due to the fact that this factor did not affect any response (Table 2).

Insert Figure 2

In the case of the response "size", although it was influenced by different factors (Table 2), in all experiments it remained between 36.3 and 390.0 nm. These size values are in the submicron range,[40] which is suitable for the preparation of NEs. Therefore, this factor was not optimized. All experiments were performed in random order to minimize the effects of uncontrolled factors that may introduce a bias on the measurements.

The responses for all the 30 experiments were fitted to polynomial models, using backward elimination to estimate the best models. These results indicated that a linear model best explains the behavior of the responses DCR (*p-value* = < 0.0001) and zeta-potential (*p-value* = 0.002), while a quadratic model was appropriate for both the association efficiency (*p-value* = < 0.0001) and PDI (*p-value* = 0.006). A 2FI model was correlated with the stability over storage (*p-value* = 0.006).

When a simple response is considered, the model analysis indicates areas in the design region where the system is likely to give desirable results. However, when several responses need to be optimized simultaneously, the desirability function, which is a function of more than one response, can be employed[41]. The desirability with a range from 0 (value undesirable) to 1 (all responses are in a desirable range simultaneously), was employed to optimize the mentioned responses simultaneously.

As reported[42], the low drug loading represent a serious drawback due to may lead to the administration of large volume of the products to produce the required biological activity. According to it, the highest importance in the optimization process was to achieve a high AE. Four responses, as suggested by the analysis of the above-discussed effect, were simultaneously optimized: minimum PDI and zeta-potential, and maximum DCR and association efficiency. During the optimization, an importance of 1+ was assigned to the responses PDI, zeta-potential and DCR while a maximum importance (5+) was assigned to association efficiency. After the optimization method was conducted, a response surface for the global desirability was built as a function of the influencing factors (Figure 3).

Insert Figure 3

A close inspection of Figure 3A reveals that both high Miglyol® 812 concentration and high log P values increased the desirability parameter, while smaller values reduced it dramatically, probably because the system becomes unstable under these conditions. Notice that the most influential factor for the association efficiency in any of the different combinations (response with the highest assigned importance) was the log P of each model drug (Figure 3B, 3C and 3D).

Therefore, based on the design presented in Table 2, three optimization conditions: log P at 2.44, 2.69 and 5.9, corresponding with PZQ, PYR and TCBZ were fixed, respectively. Both PYR and PZQ were selected because both drugs have low log P values that were associated to smaller desirability and association efficiency. Then, the responses were

optimized in the worst working conditions. The desirability and different responses as function of the factors for each selected log P value are shown in Figure 4.

Insert Figure 4.

As expected, the maximum desirability value (0.94) was obtained when log P value was 5.9 (for TCBZ) while desirability values of 0.82 and 0.80 were obtained for log P values of 2.44 and 2.69, respectively. Desirability plots for PZQ, PYR and TCBZ showed that this function was improved when the Miglyol® 812 concentration was highest. When low log P values were analyzed (2.44 and 2.69) it was observed that at the lowest Miglyol® 812 concentration the desirability function was zero. Miglyol® 812 is the oil phase of the nanoemulsion where the drug is dissolved and the log P value measures the capacity of a drug to be solubilized in the organic phase. Thus, the lower log P value, the lower its solubility in this phase. Therefore, the lowest log P values and lowest Miglyol® 812 concentration afforded the lowest desirability. As expected, it was also observed that the association efficiency was improved when highest Span® 80 concentrations were employed. Based on the obtained desirability functions, the best working conditions corresponding to the design (which is in the region of maximum desirability) were selected. The desirability function yielded values of D=0.82 (log P=2.44) using the following factor values: Miglyol® 812: 350 µL, lecithin: 120 mg, and Span® 80: 0.09 mg; D=0.80 (log P=2.69), using the following factors values Miglyol® 812: 350 µL, lecithin: 120 mg, and Span® 80: 0.43 mg; and D=0.94 (log P=5.9), using the following factors values Miglyol® 812: 340 µL, lecithin: 95 mg, and Span® 80: 0.9 mg, which were suitable for the purposes of this work.

3.3 Experimental verification

The optimal conditions for the preparation of NEs were verified by an additional independent experiment (Table 4).

Insert Table 4.

The obtained results were in close agreement with the predicted optimum values, with slight differences related to the measurement error. These interesting findings provided strong confidence that the applied optimization procedure led to reliable values of the factors influencing the presently studied formulation. Some of the optimum factor values could be explained by considering the physicochemical parameters of the formulated NEs, as discussed before.

4. Conclusions

This work demonstrates that several widely used hydrophobic drugs in human and veterinary medicine were successfully loaded in stabilized NEs through the rational analysis of different parameters involved in the formulations. Miglyol® 812, as oil phase, and soybean lecithin and Span® 80 as co-surfactants lead to stable O/W NEs, which exhibited particle sizes lower than 160 nm and an association efficiency between 55 and 97%. Both the mixing order and the Span® 80 concentration played a fundamental role in the polydispersion index and the

storage stability, respectively. Particularly, the optimization of stabilized NEs loaded with praziquantel (presenting 97% of association efficiency) and with pyrimetamine (presenting 92% of association efficiency) was successfully done. Thus, these stable NEs based on Miglyol® 812, soybean lecithin and Span® 80 are a promising approach for potential treatment of different neglected parasitic diseases.

5. Conflicts of interest

There are no conflicts to declare.

6. Funding and Acknowledgements

This project has received funding from the European Union's Seventh Framework Programme for research, technological development and demonstration under grant agreement N°613931. We gratefully acknowledge support from PROALAR (DA/13/08 Project, DAAD-MINCyT International cooperation). DR, DL, and CJS gratefully acknowledge the Universidad Nacional de Rosario (Argentina), MINCyT (Argentina) and CONICET (Argentina) for financial support. DR thanks CONICET (Argentina) for a Ph.D. fellowship.

7. References

[1] N.K. Sachan, A. Bhattacharya, S. Pushkar, A. Mishra, Biopharmaceutical classification system: A strategic tool for oral drug delivery technology, Asian J. Pharm. 3 (2009) 76–81. https://doi.org/10.4103/0973-8398.55042.

[2] Y. Kawabata, K. Wada, M. Nakatani, S. Yamada, S. Onoue, Formulation design for poorly water-soluble drugs based on biopharmaceutics classification system:

Basic approaches and practical applications, Int. J. Pharm. 420 (2011) 1–10. https://doi.org/10.1016/j.ijpharm.2011.08.032.

[3] S.M. Abuzar, S.M. Hyun, J.H. Kim, H.J. Park, M.S. Kim, J.S. Park, S.J. Hwang, Enhancing the solubility and bioavailability of poorly water-soluble drugs using supercritical antisolvent (SAS) process, Int. J. Pharm. 538 (2018) 1–13. https://doi.org/10.1016/j.ijpharm.2017.12.041.

[4] S. Saad, I. Ahmad, S.M. Kawish, U.A. Khan, G.K. Jain, Improved cardioprotective effects of hesperidin solid lipid nanoparticles prepared by supercritical antisolvent technology, Colloids Surf B Biointerfaces 187 (2020), 110628. https://doi.org/10.1016/j.colsurfb.2019.110628

[5] J. Zhang, Y. Huang, D. Liu, Y. Gao, S. Qian, Preparation of apigenin nanocrystals using supercritical antisolvent process for dissolution and bioavailability enhancement, Eur. J. Pharm. Sci. 48 (2013) 740–747. https://doi.org/10.1016/j.ejps.2012.12.026.

[6] K. Ueda, K. Higashi, K. Moribe, Mechanistic elucidation of formation of drug-rich amorphous nanodroplets by dissolution of the solid dispersion formulation, Int. J. Pharm. 561 (2019) 82–92. https://doi.org/10.1016/j.ijpharm.2019.02.034.

[7] D. Real, L. Orzan, D. Leonardi, C.J. Salomon, Improving the Dissolution of Triclabendazole from Stable Crystalline Solid Dispersions Formulated for Oral Delivery, AAPS PharmSciTech. 21 (2020) 16. https://doi.org/10.1208/s12249-019-1551-4.

[8] Q. Fu, B. Li, D. Zhang, M. Fang, J. Shao, M. Guo, Z. Guo, M. Li, J. Sun, Y. Zhai, Comparative studies of the in vitro dissolution and in vivo pharmacokinetics for different formulation strategies (solid dispersion, micronization, and nanocrystals) for poorly water-soluble drugs: A case study for lacidipine. Colloids Surf. B Biointerfaces 132 (2015) 171-176. https://doi:10.1016/j.colsurfb.2015.05.010

[9] D. Real, D. Leonardi, R.O. Williams, M.A. Repka, C.J. Salomon, Solving the Delivery Problems of Triclabendazole Using Cyclodextrins, AAPS PharmSciTech. 19 (2018) 2311–2321. https://doi.org/10.1208/s12249-018-1057-5.

[10] N. Liu, K. Higashi, K. Ueda, K. Moribe, Effect of guest drug character encapsulated in the cavity and intermolecular spaces of γ-cyclodextrins on the dissolution property of ternary γ-cyclodextrin complex, Int. J. Pharm. 531 (2017) 543–549. https://doi.org/10.1016/j.ijpharm.2017.04.049.

[11] A. García, J. Priotti, A.V. Codina, M.D. Vasconi, A.D. Quiroga, L.I. Hinrichsen, D. Leonardi, M.C. Lamas, Synthesis and characterization of a new cyclodextrin derivative with improved properties to design oral dosage forms, Drug Deliv. Transl. Res. 9 (2019) 273–283. https://doi.org/10.1007/s13346-018-0591-8.

[12] H.F. Santos Souza, D. Real, D. Leonardi, A.M. Silber, C.J. Salomon, Development and in vitro/in vivo evaluation of a novel benznidazole liquid dosage form using a quality-by-design approach, Trop. Med. Int. Heal. 22 (2017) 1514–1522. https://doi.org/10.1111/tmi.12980.

[13] M. Morri, P. Castellano, D. Leonardi, S. Vignaduzzo, First development, optimization, and stability control of a pediatric oral atenolol formulation, AAPS PharmSciTech. 19 (2018) 1781–1788. https://doi.org/10.1208/s12249-018-0992-5.

[14] M.K. Yeh, L.C. Chang, A.H.J. Chiou, Improving tenoxicam solubility and bioavailability by cosolvent system, AAPS PharmSciTech. 10 (2009) 166–171. https://doi.org/10.1208/s12249-009-9189-2.

[15] A.A. Sharipova, S.B.Aidarova, D.Grigoriev, B.Mutalieva, G.Madibekova, A.Tleuova, R.Miller, Polymer–surfactant complexes for microencapsulation of vitamin E and its release, Colloids Surf. B Biointerfaces 1371 (2016) 152-157. https://doi.org/10.1016/j.colsurfb.2015.03.063.

[16] M.A. Alhnan, S. Murdan, A.W. Basit, Encapsulation of poorly soluble basic drugs into enteric microparticles: A novel approach to enhance their oral bioavailability, Int. J. Pharm. 416 (2011) 55–60. https://doi.org/10.1016/j.ijpharm.2011.05.079.

[17] A. García, D. Leonardi, G.N. Piccirilli, M.E. Mamprin, A.C. Olivieri, M.C. Lamas, Spray drying formulation of albendazole microspheres by experimental design. In vitro - In vivo studies, Drug Dev. Ind. Pharm. 41 (2015) 244–252. https://doi.org/10.3109/03639045.2013.858737.

[18] K. Göke, T. Lorenz, A. Repanas, F. Schneider, D. Steiner, K. Baumann, H. Bunjes, A. Dietzel, J.H. Finke, B. Glasmacher, A. Kwade, Novel strategies for the formulation and processing of poorly water-soluble drugs, Eur. J. Pharm. Biopharm. 126 (2018) 40–56. https://doi.org/10.1016/j.ejpb.2017.05.008.

[19] P. Sahu, D. Das, V.K. Mishra, V. Kashaw, S.K. Kashaw, Nanoemulsion: A Novel Eon in Cancer Chemotherapy, Mini-Reviews Med. Chem. 17 (2016). https://doi.org/10.2174/1389557516666160219122755.

[20] S. Yadav, S.K. Gandham, R. Panicucci, M.M. Amiji, Intranasal brain delivery of cationic nanoemulsion-encapsulated TNFα siRNA in prevention of experimental neuroinflammation, Nanomedicine Nanotechnology, Biol. Med. 12 (2016) 987–1002. https://doi.org/10.1016/j.nano.2015.12.374.

[21] J. Desai, H. Thakkar, Enhanced oral bioavailability and brain uptake of Darunavir using lipid nanoemulsion formulation, Colloids and Surf. B: Biointerfaces 1751 (2019) 143-149. https://doi.org/10.1016/j.colsurfb.2018.11.057.

[22] M.C. Vinaud, D. Real, C.M. Fraga, N.F. Lima, R. De Souza Lino Junior, D. Leonardi, C. J. Salomon, Nanodelivery of nitazoxanide: impact on the metabolism of *Taenia crassiceps* cysticerci intracranially inoculated in mice, Ther. Deliv. (2020) tde-2020-0017. https://doi.org/10.4155/tde-2020-0017.

[23] J. Akhtar, H.H. Siddiqui, Badruddeen, S. Fareed, M. Aqil, Nanomulsion as a Carrier for Efficient Delivery of Metformin, Curr. Drug Deliv. 11 (2014) 243–252. https://doi.org/10.2174/1567201811102140411160817.

[24] G.Calderó, R.Montes, M.Llinàs, M.J.García-Celma, M.Porras, C.Solans, Studies on

the formation of polymeric nano-emulsions obtained via low-energy emulsification and their use as templates for drug delivery nanoparticle dispersions, Colloids and Surf. B: Biointerfaces 145 (2016), 922-931. https://doi.org/10.1016/j.colsurfb.2016.06.013.

[25] A. Azeem, M. Rizwan, F.J. Ahmad, Z. Iqbal, R.K. Khar, M. Aqil, S. Talegaonkar, Nanoemulsion components screening and selection: A technical note, AAPS PharmSciTech. 10 (2009) 69–76. https://doi.org/10.1208/s12249-008-9178-x.

[26] M. Kaiser, B. Kirsch, H. Hauser, D. Schneider, I. Seuß-Baum, F.M. Goycoolea, In Vitro and Sensory Evaluation of Capsaicin-Loaded Nanoformulations, PLoS One. 10 (2015) e0141017. https://doi.org/10.1371/journal.pone.0141017.

[27] C. Prego, D. Torres, M.J. Alonso, Chitosan nanocapsules as carriers for oral peptide delivery: effect of chitosan molecular weight and type of salt on the in vitro behaviour and in vivo effectiveness., J. Nanosci. Nanotechnol. 6 (n.d.) 2921–8. http://www.ncbi.nlm.nih.gov/pubmed/17048499 (accessed June 5, 2019).

[28] F. Maestrelli, P. Mura, M.J. Alonso, Formulation and characterization of triclosan sub-micron emulsions and nanocapsules, J. Microencapsul. 21 (2004) 857–864. https://doi.org/10.1080/02652040400015411.

[29] P. Calvo, C. Remuñán-López, J.L. Vila-Jato, M.J. Alonso, Development of positively charged colloidal drug carriers: Chitosan-coated polyester nanocapsules and submicron-emulsions, Colloid Polym. Sci. 275 (1997) 46–53. https://doi.org/10.1007/s003960050050.

[30] D. Real, S. Hoffmann, D. Leonardi, C. Salomon, F.M. Goycoolea, Chitosan-based nanodelivery systems applied to the development of novel triclabendazole formulations, PLoS One. 13 (2018) 115–135. https://doi.org/10.1371/journal.pone.0207625.

[31] D. Leonardi, M.C. Lamas, A.C. Olivieri, Multiresponse optimization of the properties of albendazole–chitosan microparticles, J. Pharm. Biomed. Anal. 48 (2008) 802–807. https://doi.org/10.1016/j.jpba.2008.08.006.

[32] T. Bastogne, Quality-by-design of nanopharmaceuticals – a state of the art, Nanomedicine Nanotechnology, Biol. Med. 13 (2017) 2151–2157. https://doi.org/10.1016/J.NANO.2017.05.014.

[33] L.X. Yu, Pharmaceutical quality by design: Product and process development, understanding, and control, Pharm. Res. 25 (2008) 781–791. https://doi.org/10.1007/s11095-007-9511-1.

[34] K. Vanaja, R.H.S. Rani, Design of experiments: Concept and applications of plackett burman design, Clin. Res. Regul. Aff. 24 (2007) 1–23. https://doi.org/10.1080/10601330701220520.

[35] World Health Organization, 20th WHO Essential Medicines List. 2017, 2017. https://www.who.int/medicines/news/2017/20th_essential_med-list/en/ (accessed June 4, 2019).

[36] F.S. Poletto, L.A. Fiel, B. Donida, M.I. Ré, S.S. Guterres, A.R. Pohlmann, Controlling the size of poly(hydroxybutyrate-co-hydroxyvalerate) nanoparticles prepared by emulsification-diffusion technique using ethanol as surface agent, Colloids Surfaces A Physicochem. Eng. Asp. 324 (2008) 105–112. https://doi.org/10.1016/j.colsurfa.2008.04.003.

[37] L. Ambrosone, A. Ceglie, G. Colafemmina, G. Palazzo, Emulsions: A time-saving evaluation of the droplets' polydispersity and of the dispersed phase self-diffusion coefficient †, Langmuir. 15 (1999) 6775–6780. https://doi.org/10.1021/la990257e.

[38] J. Rao, D.J. McClements, Stabilization of phase inversion temperature nanoemulsions by surfactant displacement, J. Agric. Food Chem. 58 (2010) 7059–7066. https://doi.org/10.1021/jf100990r.

[39] G. Hanrahan, K. Lu, Application of factorial and response surface methodology in modern experimental design and optimization, Crit. Rev. Anal. Chem. 36 (2006) 141–151. https://doi.org/10.1080/10408340600969478.

[40] K. Shanmugapriya, H. Kim, P.S. Saravana, B-S. Chun, H.W. Kang, Astaxanthin-alpha tocopherol nanoemulsion formulation by emulsification methods: Investigation on anticancer, wound healing, and antibacterial effects, Colloids and Surf. B: Biointerfaces 1721 (2018) 170-179. https://doi.org/10.1016/j.colsurfb.2018.08.042.

[41] L. Vera Candioti, M.M. De Zan, M.S. Cámara, H.C. Goicoechea, Experimental design and multiple response optimization. Using the desirability function in analytical methods development, Talanta. 124 (2014) 123–138. https://doi.org/10.1016/j.talanta.2014.01.034.

[42] J. Rao, D.J. McClements, Food-grade microemulsions and nanoemulsions: Role of oil phase composition on formation and stability, Food Hydrocoll. 29 (2012) 326–334. https://doi.org/10.1016/j.foodhyd.2012.04.008.

CRediT authorship contribution statement

Daniel A. Real: Conceptualization, Methodology, Software, Validation, Formal analysis, Investigation, Writing - original draft, Visualization, Project administration. Stefan Hoffmann Stefan: Conceptualization, Validation, Formal analysis, Investigation, Writing - original draft. Darío Leonardi: Conceptualization, Software, Validation, Formal analysis, Investigation, Data curation, Writing - review & editing, Project administration. Francisco M. Goycoolea: Funding acquisition, Resources, Writing - review & editing, Conceptualization, Validation, Formal analysis, Data curation, Project administration, Supervision. Claudio J. Salomon: Funding acquisition, Resources, Writing - review & editing, Conceptualization, Validation, Formal analysis, Data curation, Supervision.

Declaration of Competing Interest

There are no conflicts to declare.

Table 1. Plackett–Burman design built for factor select

	Factors										Responses					
Run	M[a]	L[b]	S80[c]	log P	Solv[d]	SR[e]	MO[f]	TBE[g]	AV[h]	FEV[i]	Size[j]	PDI[k]	DCR[l]	AE[m]	PBS_{sr}[n]	St30[o]
1	250	40	1	0.91	E	500	O-W	30	10	10	464.4	0.186	50,514.8	12.7	0.78	1005
2	250	40	1	0.91	A	0	W-O	1	20	10	254.0	0.311	52,318.7	9.6	0.82	1000
3	250	80	0	0.91	E	0	O-W	30	20	7	222.8	0.163	175,426.7	8.7	0.93	0,583
4	250	80	0	5.90	E	500	W-O	1	10	10	212.6	0.151	101,454.6	90.6	2.13	1262
5	250	80	1	5.90	A	0	O-W	1	10	7	187.0	0.192	86,598.6	86.2	0.96	1488
6	125	40	1	5.90	E	500	O-W	1	20	7	177.8	0.242	65,770.3	83.3	0.85	0,966
7	125	80	1	5.90	E	0	W-O	30	20	10	187.4	0.349	33,427.5	51.8	0.70	0,445
8	125	80	0	0.91	A	500	O-W	1	20	10	213.2	0.331	26,343.3	8.0	0.88	0,714
9	125	40	0	0.91	E	0	W-O	1	10	7	162.8	0.318	35,356.0	7.9	0.90	1491
10	250	40	0	5.90	A	500	W-O	30	20	7	383.1	0.349	49,725.4	89.9	2.31	0,863
11	125	80	1	0.91	A	500	W-O	30	10	7	88.5	0.510	4879.7	11.2	0.63	2587
12	125	40	0	5.90	A	0	O-W	30	10	10	239.2	0.290	88,331.9	76.7	1.92	0,824

[a] Miglyol® 812.
[b] Lecithin.
[c] Spam 80.
[d] Solvent (Ethanol and Acetone).
[e] Stirring rate.
[f] Mixing order.
[g] Time before evaporation.
[h] Aqueous volume.
[i] Final evaporation volume.
[j] Particle size.
[k] Polydispersion index.
[l] Derived count rate.
[m] Association efficiency.
[n] Phosphate-buffered saline.
[o] Stability storage time.

Table 2. p-values for the different factors of the six responses

	Size	PDI[e]	DCR[f]	AE[g]	PBS_{St}[h]	ST30[i]
Model	0.0432	0.0108	0.0070	0.0038	0.0045	0.0438
Miglyol® 812	0.0181	0.0035	0.0020	0.0682	0.0765	–
Lecithin	0.0298	–	–	–	–	–
Span® 80	–	0.0444	–	0.2897	0.0031	0.1299
Log P	–	0.0267	–	0.0003	0.0052	0.1718
Solvent	–	0.0051	0.0077	0.2946	–	0.1351
Stirring time	0.1907	0.0706	–	0.0808	0.2094	0.1649
MO[a]	0.3057	0.0049	0.0034	–	–	0.0884
TBE[b]	0.1023	0.0179	0.0541	0.1992	–	–
AV[c]	–	0.1394	0.2069	0.2037	–	0.0115
FEV[d]	0.1248	0.0627	–	0.1702	–	0.0417

The outlier point was remove for the analysis of the model.

[a] Mixing order.
[b] Time before evaporation.
[c] Aqueous volume.
[d] Final evaporation volume.
[e] Polydispersion index.
[f] Derived count rate.
[g] Association efficiency.
[h] Phosphate-buffered saline.
[i] Stability storage time.

Table 3. Central composite design used for the optimization of the responses.

	Factors					Responses					
std	Run	M[a]	L[b]	S80[c]	log P	Size[d]	PDI[e]	ZP[f]	AE[g]	DCR[h]	ST30[i]
17	1	0.00	42	1	4.49	399.0	0.363	−28.9	3.63	67,978.3	0,276
7	2	12.50	80	2	2.69	52.7	0.149	−27.7	27.01	439.6	0,569
5	3	12.50	4	2	2.69	202.1	0.247	−29.6	18.85	1007.1	1187
14	4	250.00	4	2	5.90	181.2	0.122	−22.8	94.95	178,522.5	1075
11	5	12.50	80	0	5.90	82.4	0.285	−41.7	90.83	15,025.9	0,798
19	6	131.25	0	1	4.49	352.5	0.529	−25.4	1.31	122,889.6	0,517
29	7	131.25	42	1	4.49	397.0	0.565	−35.0	1.92	73,060.3	0,316
9	8	12.50	4	0	5.90	147.7	0.081	−27.3	65.33	110,592.4	0,848
21	9	131.25	42	0	4.49	164.4	0.224	−40.6	2.47	55,871.0	1088
4	10	250.00	80	0	2.69	159.1	0.178	−42.7	11.86	133,452.6	12,320
3	11	12.50	80	0	2.69	80.7	0.279	−32.5	10.33	4218.9	8470
23	12	131.25	42	1	0.91	152.2	0.233	−48.4	10.48	71,255.2	0,992
10	13	250.00	4	0	5.90	213.3	0.08	−38.4	95.59	171,997.9	1092
12	14	250.00	80	0	5.90	172.6	0.18	−46.7	90.50	201,347.0	0,954
28	15	131.25	42	1	4.49	287.3	0.474	−30.7	1.71	55,609.9	0,450
13	16	12.50	4	2	5.90	176.1	0.112	−22.2	93.33	62,721.1	0,380
27	17	131.25	42	1	4.49	182.8	0.442	−33.8	1.52	72,056.0	0,793
24	18	131.25	42	1	2.44	152.3	0.192	−43.5	0.00	68,135.9	0,986
26	19	131.25	42	1	4.49	295.5	0.472	−39.9	1.92	85,007.1	0,490
6	20	250	4	2	2.69	192.4	0.130	−17.3	18.13	162,538.1	1200
16	21	250	80	2	5.90	159.1	0.198	−32.5	96.95	162,632.2	0,928
15	22	12.5	80	2	5.90	36.3	0.380	−30.3	87.91	1529.3	1439
20	23	131.25	118	1	4.49	183.2	0.264	−45.7	54.23	50,716.4	0,524
25	24	131.25	42	1	4.49	156.7	0.389	−42.9	1.74	48,557.5	0,854
2	25	250	4	0	2.69	220.9	0.127	−32.3	5.46	117,542.7	2350
18	26	368.75	42	1	4.49	202.6	0.250	−37.0	2.78	206,928.5	1103
8	27	250	80	2	2.69	164.6	0.147	−29.0	29.67	129,082.4	1149
22	28	131.25	42	3	4.49	216.7	0.476	−33.9	2.87	51,651.7	0,672
30	29	131.25	42	1	4.49	169.8	0.271	−28.5	0.00	73,275.6	0,833
1	30	12.5	4	0	2.69	140.9	0.240	−29.9	2.17	7211.0	1201

[a] Miglyol® 812.
[b] Lecithin.
[c] Spam 80.
[d] Particle size.
[e] Polydispersion index.
[f] Zeta potential.
[g] association efficiency.
[h] Derived count rate.
[i] Stability storage time.

Table 4. Summary of physical characteristics of PZQ (log P = 2.44), PYR (log P = 2.69) and TCBZ (log P = 5.9) optimized nanoemulsions

Drug (log P)	Response	Predicted value	Experimental value[a]
PZQ (2.44)	Size	–	146.9
	AE[b]	96.18	97.03
	ZP[c]	−56.6	−48.3
	PDI[d]	0.25	0.18
	DCR[e]	110,269.6	119,970.5
	ST30[f]	–	0.976
PYR (2.69)	Size	–	144.83
	AE[b]	64.84	55.88
	ZP[c]	−35.56	−32.70
	PDI[d]	0.25	0.19
	DCR[e]	104,021.1	106,122.2
	ST30[f]	–	1.120
TCBZ (5.9)	Size	–	154.76
	AE[b]	94.79	92.58
	ZP[c]	−46.8	−48.0
	PDI[d]	0.20	0.18
	DCR[e]	232,314.8	230,379.5
	ST30[f]	–	0.987

[a] All the experiments were done in triplicate ($n = 3$).
[b] Association efficiency.
[c] Zeta potential.
[d] Polydispersion index.
[e] Derived count rate.
[f] Stability storage time.

Figure 1.
Influence of solvent type,mixing order, Span 80,Miglyol and Lecithin. One factor graphs showing the effect of ethanol and acetone over polidispersión index (A) and derived count rate (B). Influence of phases mixing order in PDI (C) and DCR (D). Effects of the factors on stability in PBS [Span® 80 (E)], PDI [Miglyol (F)] and size [Miglyol (G) and Lecithin (H)].

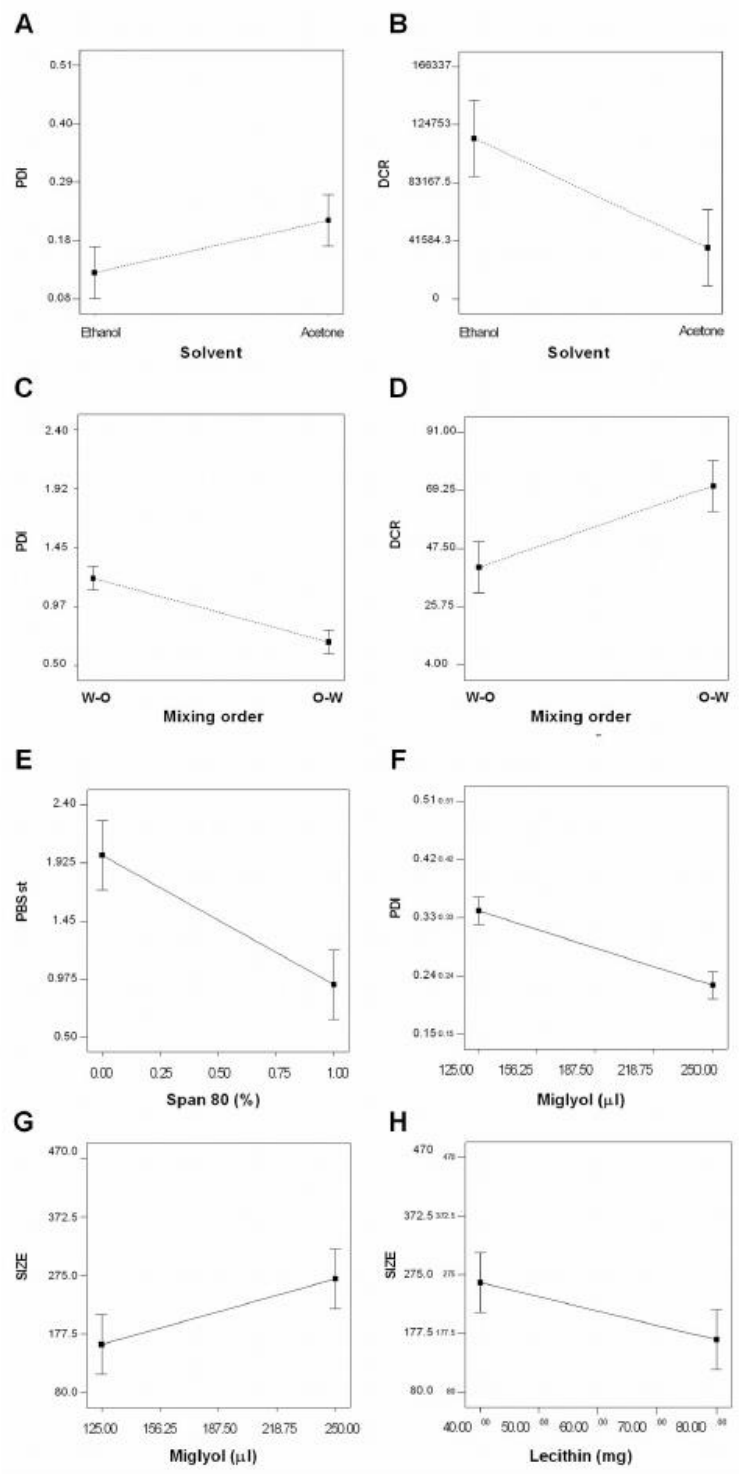

Figure 2. Influence of time before evaporation, aqueous volume and final evaporation volume. One factor graphs showing the effect of the factors on PDI (time before evaporation [A]) and ST30 (aqueous volume [B] and final evaporation volume [C]).

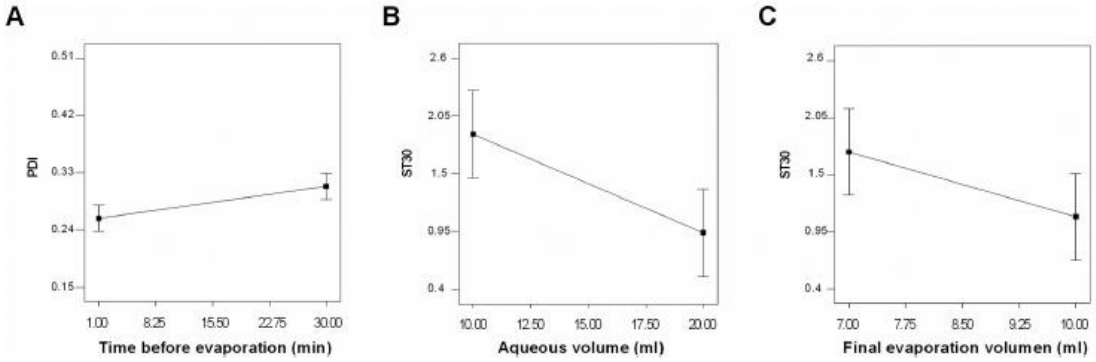

Figure 3. Global desirability and association efficiency as function of different factors. Response surface graphs showing the effect of log P andMiglyol over desirability [A], and the influence of log P over association efficiency at different concentrations of lecithin [B], Miglyol [C] and Span 80 [D].

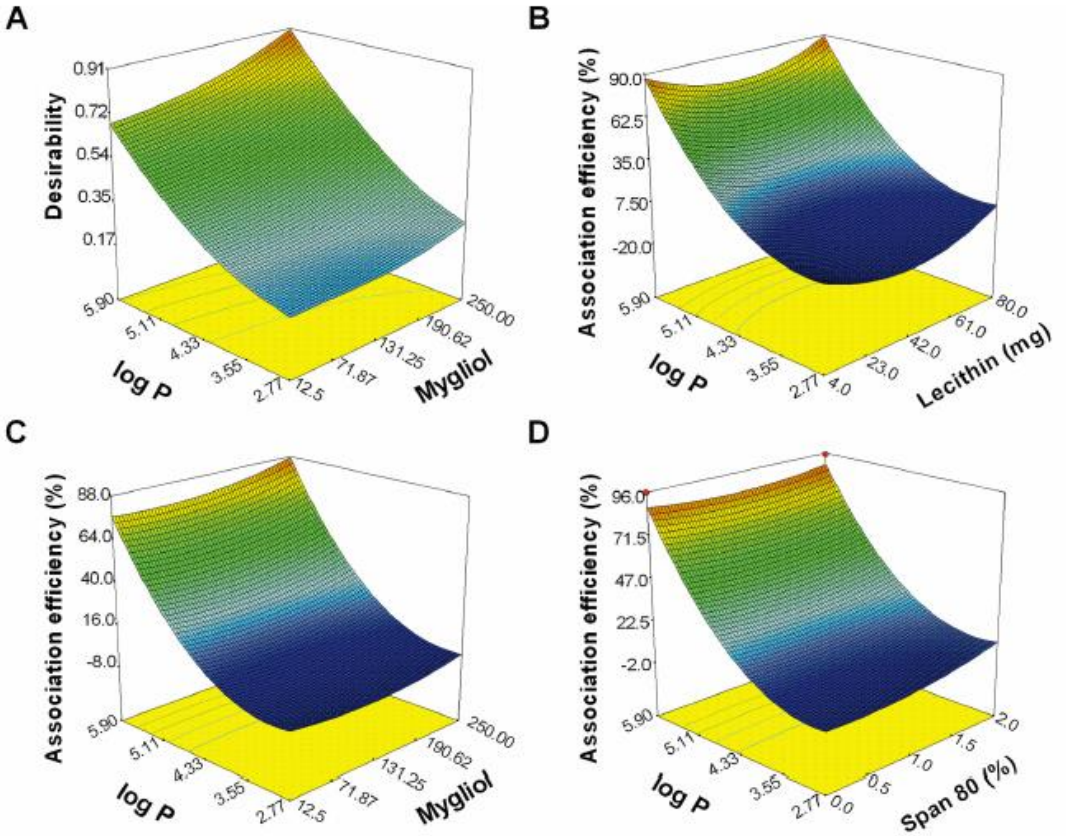

Figure 4. Desirability and responses as functions of factors for each selected log P values. Response surface graphs of desirability, association efficiency, PDI, Z-pot and DCR for differents log P values. Column A: log P = 2.44 (Praziquantel), column B: log P = 2.99 (Pyrimethamine), column C: log P = 5.9 (Triclabendazole).